AJ ACADEMIC JOURNALS
expand your knowledge

Journal of Chemical Engineering and Materials Science

Full Length Research Paper

Effect of plasma magnet power supplies operating temperatures on the thermal life of space-vehicles

A. Anvari

Department of Mechanical and Aerospace Engineering, University of Missouri-Columbia, Columbia, Missouri, U.S.A.

The galactic and solar radiation effect on astronauts in space during manned-space missions is one of the issues that scientists are dealing with to overcome this disaster. Furthermore, in space missions to Mars, Titan, and beyond, a powerful propulsion system is required. Recently, with the enhancement of technology in plasma generation, scientists tried to design and build a plasma radiation shield and plasma propulsion system to create a safe and reliable space-craft for long-term space missions. In the present research, an attempt is made to estimate the thermal fatigue life of unidirectional carbon fiber/epoxy composite in the presence of plasma radiation shield and/or plasma propulsion systems. In order to produce a plasma radiation shield and/or plasma propulsion system, a strong magnet that generates a magnetic field for electron cloud is required. For charging magnets, appropriate power supplies are needed. Each of the different power supplies has different operating temperatures that have effect on the thermal fatigue life of space-vehicles structure. In this study, with a new method, thermal fatigue life of unidirectional carbon fiber/epoxy composite which is exposed to different power supplies thermal cycles is predicted. The results have indicated that the new method represents 32.2 % less thermal fatigue life when compared to the previous method. Space-crafts are currently being built with carbon materials such as unidirectional carbon fiber/epoxy composite, due to their lightweights and high strength.

Key words: Plasma shield, plasma propulsion, power supply, astronauts' health, composites, thermal fatigue life.

INTRODUCTION

Thermal fatigue life of unidirectional carbon fiber/epoxy

Thermal fatigue life of Unidirectional Carbon Fiber/Epoxy Composite (UD CF/EP) in Low Earth Orbit (LEO) has been analyzed previously (Anvari, 2014). As Mars appears to be the closest planet to Earth in the solar system, the thermal fatigue life of UD CF/EP on Mars was investigated in 2017 (Anvari, 2017a). Furthermore, it is important to note that due to the similarity and closeness of Mars to Earth, one-way human mission to Mars was proposed (Schulze-Makuch and Davies, 2010). Moreover, due to the characteristics of the atmosphere of Titan, Saturn's moon, which is a great shield against solar and cosmic radiation and being safe in this aspect for human-life, thermal fatigue life of UD CF/EP in Titan

E-mail: aabm9@mail.missouri.edu.

was provided in 2018 (Anvari, 2018).

It is significant to mention that using Bidirectional Carbon Fiber/Epoxy Composite (BD CF/EP) for building space-vehicles is not recommended. This is because based on previous research (Anvari, 2017b), the crack growth rate due to temperature variation in BD CF/EP is approximately 170 times of that in UD CF/EP. Thus, employing BD CF/EP in space-vehicles structures could expose the crew lives and space-vehicles' structures' integrity and safety to risk of space-craft's thermal failure. On the other hand, application of CNT wire in space-vehicles' structures is recommended (Anvari, 2017c) because CNT wire thermal tolerance strength in varied temperatures is about 10% higher than that for UD CF/EP. Hence, space-vehicles' structures built with CNT wire last close to 10% in relation to higher thermal fatigue cycle numbers to failure compared to those built with UD CF/EP.

With the investigation of manned-space missions, it is obvious that one of the major issues in manned-space missions is the radiation effects on astronauts. This problem exists during the space-travel. Furthermore, this issue does not just exist in space or beyond the Earth Orbit. This problem also exists in some planets such as Mars. Because Mars' atmosphere has a very small thickness in comparison with the Earth's atmosphere (Pasachoff, 1993), it is not capable to build an adequate shield against solar and cosmic radiation. As a result, it is considered as a health-risk for crew such as possibility of causing cancer, other illnesses, and even death in worst cases (Cucinotta et al., 2005; Horneck and Comet, 2006).

Currently, it has been discovered that plasma technology can be applied in space-vehicles to solve radiation effects issues for astronauts by eliminating the radiation effects in space-missions (Diaz and Seedhouse, 2017). Even the application of plasma technology in space-crafts can generate high-power propulsion system for future space-missions to Mars and beyond (Diaz and Seedhouse, 2017). It is important to mention that this harmful radiation effect is caused by solar and/or galactic radiation events such as solar wind event emitting from the sun. Therefore, this effect is initiated from the space environment.

To use the plasma technology in space-vehicles, there would be some requirements such as some components to attach to space-crafts for operating the plasma within the space-missions. These components are included but not limited to magnet that creates the magnetic field for the electron cloud that creates shield against the solar and cosmic radiation, and power supplies such as fuel cells to empower or charge the magnet. There are many kinds of power supplies that can be used to charge the magnet during the space missions to generate the radiation shield. Each of these power supplies has different operating temperatures. Hence, when the magnet is put on to activate the radiation shield, the temperature of space vehicle is affected by this operating temperature. On the other hand, when the magnet is put

off, the temperature of the space-craft will tend to the temperature of the space environment. Consequently, thermal cycles will be created. These thermal cycles have effect on the thermal fatigue life of the space-vehicles structures. Many space-vehicles are currently built with carbon materials. Hence, the goal of this research is to investigate the effect of different magnet power supplies thermal cycles on space-vehicles thermal fatigue life. Figures 1 and 2 show the schema representing the plasma radiation shield applied in space-vehicles (CNN: Dave Gilbert, July 2, 2013). In this study, the aim is to predict the thermal fatigue life of UD CF/EP subjected to different plasma magnet power supplies thermal cycles.

There are many researches related to the evaluation of the effect of thermal cycles on mechanical properties of materials (Park et al., 2012; Shin et al., 2000; Giannadakis and Verna, 2009). Nevertheless, it appears that there is no study on the thermal fatigue life of carbon structures containing different fuel cells.

In the presented study, with modifying analytical methods obtained in 2017 (Anvari 2017), new relations are presented to predict the thermal fatigue life of UD CF/EP which is exposed to plasma magnet power supply thermal cycle. UD CF/EP can be applied in space structures subjected to different kind of plasma magnet fuel cells to generate plasma as a radiation shield and/or propulsion. The magnet power supply to generate the plasma can be attached to the outer surface of space structure to create a plasma shield at outer surface of the space craft in space.

Radiation and its effects on human health

Space-missions beyond the Earth orbit may be exposed to Galactic Cosmic Rays (GCRs) and/or Solar Particle Events (SPEs) from solar flares. These space incidents are contained with high-energy particles with high-velocity which are capable to penetrate most of the materials, including human-body tissues. Consequently, these particles can shred genetic material and cause many illness-symptoms. At high dosage, these radiation particles may result in cancer and even death of the astronauts. Scientists estimated that radiation absorption during the mission to Red planet could increase the risk of cancer for crew by maximum 5% (Diaz and Seedhouse, 2017). Therefore, the aim in this research is to predict the thermal fatigue life of UD CF/EP which is exposed to the thermal cycles generated by plasma magnet power supply at exterior surface of space craft to apply as a radiation shield and/or propulsion system.

Plasma radiation shield and propulsion system

In space missions, space-crafts are exposed to protons which have been released from solar flares. In order to
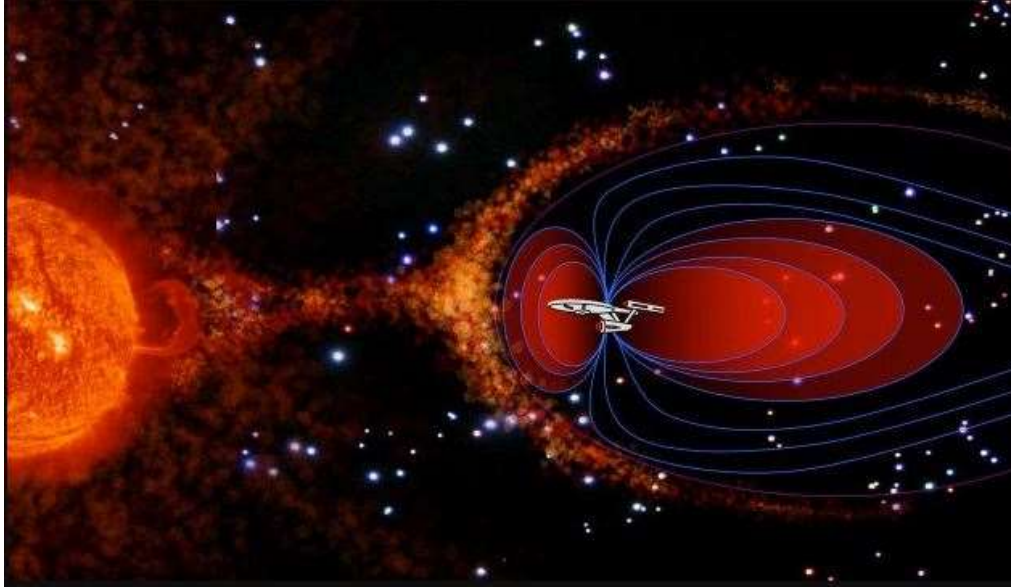
Figure 1. Schematic of the plasma radiation shield applied in space-vehicle encountering solar flare.
Source: CNN: Dave Gilbert, July 2, 2013.

Figure 2. Schematic of the plasma radiation shield applied in space-vehicle in space.
Source: CNN: Dave Gilbert, July 2, 2013.

prevent these protons from harming the astronauts' health, the concept of Plasma Radiation Shield has been introduced. However, for generating such a radiation shield with plasma to protect the space-crafts from protons emitted from solar-flare incidents, many factors are required to be considered. These factors may include but not limited to (Levy and French, 1968):

(1) Appropriate design
(2) Adequate magnetic field

(3) Equilibrium of electron cloud in dynamic level
(4) Amount of solid shield such as AluminIum
(5) Operational limitations such as in different propulsion conditions and the number of times that plasma radiation shield can be on and off during the space mission
(6) Selection of appropriate magnet charging power supply
(7) The effect of plasma radiation shield on communication systems
(8) Operational procedures for propulsion systems while

plasma radiation shield is on
(9) The effect of plasma radiation protection system on crew and their life support
(10) The effect of plasma radiation shield system on electronic equipment
(11) The weight of the magnet system for generating plasma radiation shield
(12) Attaining enough voltages and electron cloud for plasma radiation shield systems' generation and stability
(13) Integration of plasma radiation protection and propulsion system into the structure of space-vehicle.

Providing radiation shield for space-crafts is to generate a magnetic field that can hold the electron cloud to build a protection system against the emitted protons. The generation of this magnetic field is possible with the application of plasma technology (Levy and French, 1967).

There are many types of magnet charging power supplies such as Hydrogen-Oxygen and Lithium-Chlorine fuel cells. Hydrogen-Oxygen fuel cells operate at 90°C while Lithium-Chlorine fuel cells operate at 650°C. Hence, it appears that the operating temperature of Hydrogen-Oxygen fuel cell is more pleasant because operating at 650°C for Lithium-Chlorine fuel cell requires special materials and coating which can tolerate this high temperature. However, in case of high-level of power and weight saving, Lithium-Chlorine fuel cells are more beneficial when compared with Hydrogen-Oxygen fuel cells (Levy and French, 1967).

Power supplies for magnet charging

To provide both manned and unmanned space-crafts with power to operate, different kinds of power supplies such as fuel cells are produced (Warshay and Prokopius, 1989; Fuel Cell Handbook, 2004; Rahman et al., 2015; Jakupca, 2018). It appears that available fuel cells and power supplies which have the potential to generate power for manned and unmanned space-vehicles are as follows:

(1) Proton Exchange Membrane fuel cell (PEM) with 4.4 to 93.3°C operating temperatures (Vasquez et al., 2017).
(2) GenCore 5B48 Hydrogen fuel cell with -40 to 46°C operating temperatures (Birek and Molitorys, 2009).
(3) Single-sided Magneto Hydrodynamic (MHD) power plant with plasma propulsion with 27°C operating temperature (Diaz and Seedhouse, 2017).
(4) Double-sided Magneto Hydrodynamic (MHD) power plant with plasma propulsion with 327°C operating temperature (Diaz and Seedhouse, 2017).
(5) Polymeric Electrolyte Membrane Fuel Cell (PEMFC) with 120°C operating temperature (Giorgi and Leccese, 2013).
(6) Direct Methanol Fuel Cells (DMFC) with 120°C operating temperature (Giorgi and Leccese, 2013).
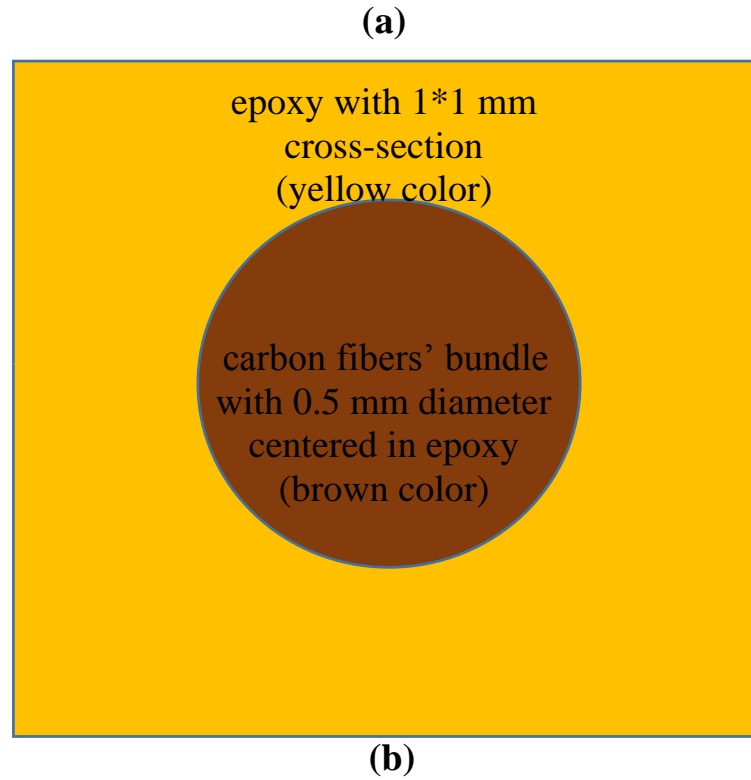(7) Alkaline Fuel Cells (AFC) with 250°C operating

temperature (Giorgi and Leccese, 2013).
(8) Phosphoric Acid Fuel Cell (PAFC) with 220°C operating temperature (Giorgi and Leccese, 2013).
(9) Molten Carbonate Fuel Cell (MCFC) with 800°C operating temperature (Giorgi and Leccese, 2013).
(10) Solid Oxide Fuel Cell (SOFC) with 1000°C operating temperature (Giorgi and Leccese, 2013).
(11) Hydrogen-Oxygen Fuel Cell with 90°C operating temperature (Levy and French, 1968).
(12) Lithium-Chlorine Fuel Cell with 650°C operating temperature (Levy and French, 1968).

It seems that application of prototype Proton Exchange Membrane (PEM) fuel cell system for up-coming manned space missions to Mars, Titan, and beyond these planets is promising. The reasons are the features of this kind of fuel cell such as low-maintenance, low-cost, and high reliability and safety requirements for future manned space-travels (Vasquez et al., 2017).

Application and properties of UD CF/EP

Advanced carbon fiber-reinforced composite laminates have been widely used in satellite structures, where the advantages of these materials-their high specific stiffness, near-zero coefficients of thermal expansion (CTE) and dimensional stabilities make them uniquely suited for applications in a low-specific-weight environment. However, since the beginning of composite structure applications, there has been a strong need to quantify the environmental effects on the composite materials based on the coupon-level laminate test data. Recent studies have shown that the environmental conditions that are the most representative of space and that tend to degrade the properties of composite laminates involve vacuum, thermal cycling atomic oxygen (AO) and micrometeoroid particles. In this respect, there is significant interest in the construction of an experimental database to capture the collective understanding of the degradation mechanisms of composite laminate in in-service environments. It is necessary to be able to predict the long-term durability of composite laminates with engineering accuracy to use these materials with confidence in critical load-bearing structures" (Park et al., 2012). The cross-section (Anvari, 2014) and material properties (Park et al., 2012; Karadeniz and Kumlutas, 2007) of UD CF/EP are illustrated and indicated in Figure 3 and Table 1, respectively. Additionally, the cross-section's dimensions and arrangement of UD CF/EP are illustrated in Figure 3a and b, respectively. It is significant to note that in Figure 3, the diameter of carbon fibers' bundle embedded in epoxy is 0.5 mm. Based on this cross-section (Anvari, 2014), the volume fraction of carbon fiber used in UD CF/EP is 19.6%. As a result, the volume fraction of epoxy in UD CF/EP is equal to 80.4%.

(a)

epoxy with 1*1 mm
cross-section
(yellow color)

carbon fibers' bundle
with 0.5 mm diameter
centered in epoxy
(brown color)

(b)

An example of arrangement of carbon fibers' bundles (brown color) in epoxy (yellow color)
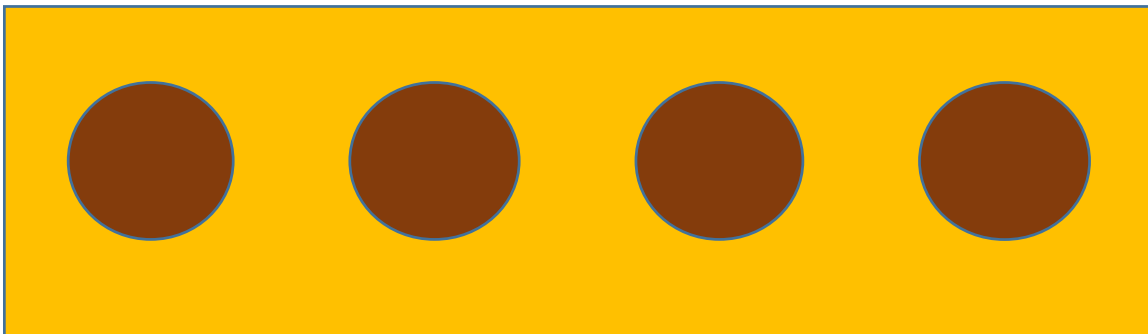
Figure 3. Cross-section of the UD CF/EP (Anvari, 2014); dimensions (a) and arrangement (b), from up to down, respectively.

Table 1. Material properties of UD CF/EP (Park et al., 2012; Karadeniz and Kumlutas, 2007).

Material	Epoxy	Carbon fiber
Axial coefficient of thermal expansion (1/^{o}C)	43.92e-6	-0.83e-6
Transverse coefficient of thermal expansion (1/^{o}C)	43.92e-6	6.84e-6
Axial Poisson's ratio	0.37	0.2
Transverse Poisson's ratio	0.37	0.4
Axial Elastic Modulus (GPa)	4.35	377
Transverse Elastic Modulus (GPa)	4.35	6.21
Axial Shear Modulus (GPa)	1.59	7.59
Transverse Shear Modulus (GPa)	1.59	2.21
Volume fraction (%)	80.4	19.6

PROBLEM FORMULATION

For estimating the thermal fatigue life of space-vehicle built with UD CF/EP which is exposed to the thermal cycles generated by different fuel cells, two methods are proposed in this study:

(1) Extended Convex Curves Method (ECCM)
(2) Compatible Steady-Linear Method (CSLM)

ECCM is the extension of Convex Curves Method (CCM) which was developed in 2014 (Anvari, 2014). Additionally, CSLM is also the modified version of Steady-Linear Method (SLM) (Anvari, 2017) (a). In the next parts of the manuscript, the procedure to derive the thermal fatigue life of UD CF/EP which is employed in space-craft structures with both ECCM and CSLM, is explained.

Extended convex curves theory

Here, the procedure to use ECCM for obtaining the thermal life of UD CF/EP exposed to the thermal cycles generated by different fuel cells is explained.

The first step is to derive the maximum thermal Inter-Laminar Shear stress ($ILSs_{max}$) imposed on UD CF/EP due to fuel cell operating temperature. The equation for calculating the $ILSs_{max}$ is indicated as (Anvari, 2018).

$$ILSs_{max} = \Delta\alpha.\Delta T_{max}.G_{max} \tag{1}$$

Equation 1 represents the $ILSs_{max}$ in axial direction (along the fibers) of fiber/matrix interface areas. In the equation, $\Delta\alpha$ is defined as $\alpha_{epoxy} - \alpha_{carbon\ fiber}$. In this study, α is the Axial Coefficient of Thermal Expansion (ACTE). The numerical values of α_{epoxy}, $\alpha_{carbon\ fiber}$, and G_{max} which is the axial shear modulus of carbon fiber are indicated in Table 1. ΔT_{max} is the maximum difference between the stress-free or crack-free temperature (23°C) and fuel cell temperature. As an instance, in Phosphoric Acid Fuel Cell (PAFC), operating temperature is -196°C (when the system is off, at minimum temperature in space (Zimcik et al., 1991)) to 220°C (when the system is on at maximum operating temperature). Hence, ΔT_{max} is equal to 23°C (UD CF/EP's stress-free temperature) minus -196°C (minimum temperature in space) which is 219°C and is the maximum temperature difference possible for this kind of fuel cell. Thus, 219°C can be substituted in Equation 1 as ΔT_{max} for PAFC. This procedure should be repeated to find ΔT_{max} for other fuel cells as well. There is no concern related to the calculation of $\Delta\alpha$ and G_{max} because it is assumed that the numerical values of α_{epoxy}, $\alpha_{carbon\ fiber}$, and G_{max} are constant. It means that they are the characteristics of UD CF/EP and do not depend on the fuel cells.

The second step is to solve the Convex Curves Equation (CCE) for Inter-Laminar Shear Strength (ILSS) (Anvari, 2014) while it is equal to $ILSs_{max}$ equation (Equation 1). Furthermore, because CCE for ILSS is related to LEO which represents 590°C temperature variation for each thermal cycle, a few changes have to be made. Equation 2 is the CCE for ILSS.

$$ILSS = (-4.87e-6) (N_{LEO})^2 + (3.84e-3) (N_{LEO}) + 80.9 \tag{2}$$

Each thermal cycle in LEO is -175°C in solar eclipse, to 120°C in sun illumination, and back to -175°C (Park et al.. 2012). Thus, each thermal cycle is 590°C in LEO. On the other hand, as an instance in PAFC, each thermal cycle is -196°C (minimum temperature in space) to 220°C (maximum operating temperature) and back to -196°C, which is 832°C. It means that each maximum thermal cycle for this fuel cell is 832°C. As a result, the following changes need to

be made in Equation 2 to obtain Equation 3 for the next step of this solution method.

$$ILSS = (-4.87e-6) (\Delta T_{FC}.N/\Delta T_{LEO})^2 + (3.84e-3) (\Delta T_{FC}.N/\Delta T_{LEO}) + 80.9 \tag{3}$$

In Equation 3, ΔT_{FC}, ΔT_{LEO}, and N, are temperature variations for fuel cell thermal cycle, temperature variation for LEO thermal cycle, and thermal cycle numbers to failure for space-vehicle containing UD CF/EP, respectively. With the substitution of the numerical values of ΔT_{FC} (for PAFC, equal to 832°C) and ΔT_{LEO} (590°C) in Equation 3, Equation 4 is obtained.

$$ILSS = (-4.87e-6) (832.N/590)^2 + (3.84e-3) (832.N/590) + 80.9 \tag{4}$$

Equation 4 is the Extended Convex Curve Equation (ECCE) of ILSS for UD CF/EP which is exposed to the thermal cycles of PAFC. Thus, by solving this equation while it is equal to Equation 1, cycle numbers to failure for UD CF/EP which is subjected to the thermal cycles of PAFC, can be derived. This relation is indicated as:

$$ILSs_{max} = ILSS\ (ECCE), \tag{5}$$

which is equal to

$$\Delta\alpha.\Delta T_{max}.G_{max} = (-4.87e-6) (832.N/590)^2 + (3.84e-3) (832.N/590) + 80.9 \tag{6}$$

With substituting the numerical values of Table 1 and ΔT_{max} for PAFC in Equation 6, Equation 7 is obtained.

$$74.4\ (MPa) = (-4.87e-6) (832.N/590)^2 + (3.84e-3) (832.N/590) + 80.9 \tag{7}$$

By solving Equation 7, cycle numbers to failure for UD CF/EP which is exposed to the thermal cycles of PAFC, is equal to 1,142 thermal cycles.

This procedure is repeated to achieve the thermal cycle numbers to failure for UD CF/EP subjected to other fuel cells thermal cycles, and the results are shown in Table 2. It is important to note that there are three different kinds of ΔT in this procedure, ΔT_{max}, ΔT_{FC} and ΔT_{LEO} which are described earlier.

Compatible steady-linear theory

Hear, deriving thermal cycle numbers to failure by the application of CSLM is explained. The first step like the ECCM is to derive the $ILSs_{max}$ using Equation 1. Prior to moving to step two, it seems necessary to mention that ILSS at zero thermal cycles for UD CF/EP ($ILSS_0$) is equal to 80.9 MPa, which is the maximum ILSS; it is used in the following equations or relations.

CSLM is divided into two parts; first, steady-region, and second, linear-region. In order to obtain the steady-region, thermal cycle numbers for this region need to be derived. The following relations could be applied to derive the thermal cycle numbers for the steady-region.

$$((ILSS_0.\Delta T_{FC})/\Delta T_{LEO}) = ILSS\ (ECCM), \tag{8}$$

which is equal to

$$((80.9.\Delta T_{FC})/\Delta T_{LEO}) = (-4.87e-6) (\Delta T_{FC}.N_{steady}/\Delta T_{LEO})^2 + (3.84e-3) (\Delta T_{FC}.N_{steady}/\Delta T_{LEO}) + 80.9 \tag{9}$$

By substituting the quantities of ΔT_{FC} and ΔT_{LEO} in Equation 9, cycle

Table 2. Thermal fatigue cycle numbers to failure (*N*) derived by ECCM and CSLM for UD CF/EP exposed to different power supplies thermal cycles.

Method\Power supplies	PEM	GenCore	MHD	PEMFC	DMFC	AFC	PAFC	Hydrogen-Oxygen
N (CSLM)	1,112	2,930	3,552	224	224	93	170	1,493
N (ECCM)	1,647	1,967	2,137	1,505	1,505	907	1,142	1,664
Difference (%)	17.6	-49	-66.2	85.1	85.1	89.8	85	10.3
Average difference (%)				32.2				

numbers for steady-region (N_{steady}) can be derived. In some circumstances, it might be impossible to derive N_{steady} due to mathematical error. In this condition, N_{steady} can be assumed as zero cycle.

For deriving the total thermal fatigue cycle numbers to failure in UD CF/EP, the following relation is employed. It is important to note that the slope in relation (Equation 10) is the average slope of Convex Curve (CC) for ILSS equation between 3000 and 4000 for LEO thermal cycles (Anvari, 2014). The reason that this slope is selected is because in this region of the convex curve the slope is approximately constant.

$$\text{ILSS}_0 = (\text{LEO CC Slope})\,(\Delta T_{FC}/\Delta T_{LEO})\,(N_{steady}) + a \quad (10)$$

In Equation 10, $ILSS_0$ as mentioned earlier is equal to 80.9 MPa. LEO CC Slope is equal to

$$- (42\ (\text{MPa}) - 15\ (\text{MPa}) / (4000\ (\text{cycles}) - 3000\ (\text{cycles}))) \quad (11)$$

Therefore, by substituting the values for LEO CC Slope in Equation 10, Equation 12 is derived.

$$80.9 = -0.027\,(\Delta T_{FC}/\Delta T_{LEO})\,(N_{steady}) + a \quad (12)$$

In this part of the procedure, by substituting the numerical values of N_{steady} which is derived from Equation 9, ΔT_{FC}, and ΔT_{LEO}, in Equation 12, the constant "a" can be derived. By deriving the numerical value of "a", the final equation to derive the cycle numbers to failure is obtained and indicated as:

$$\text{ILSs}_{max} = -0.027\,(\Delta T_{FC}/\Delta T_{LEO})\,(N) + a$$

In Equation 13, the numerical values for $ILSs_{max}$, ΔT_{FC}, ΔT_{LEO}, and "a" are already derived or available. Thus, the value of *N* which is the thermal fatigue cycle numbers to failure for UD CF/EP can be derived. This process has been performed for all the power supplies with operating temperature less than 261°C, and thermal fatigue cycle numbers to failure for UD CF/EP which is exposed to different power supplies thermal cycles derived from CSLM and ECCM; the results are indicated and shown in Table 2 and Figure 4, respectively.

It is important to mention that the temperature 261°C is the failure temperature for UD CF/EP obtained from Equation 1; while it is equal to $ILSS_0$ (with maximum inter-laminar shear strength which is equal to 80.9 MPa), by substituting the numerical values from Table 1, and stress-free temperature equal to 23°C. This procedure used to calculate the failure temperature for UD CF/EP with Equation 1 is indicated in Equation 14. In Equation 14, T_f is the failure temperature for UD CF/EP.

$$80.9\ (\text{MPa}) = (43.92 - (-0.83))\text{e-6}.(T_f - 23).(7.59\text{e+}9) \quad (12)$$

RESULTS AND DISCUSSION

As it is indicated and shown in Table 2 and Figure 4, respectively, thermal fatigue cycle numbers to failure for UD CF/EP containing MHD are the highest for both ECCM and CSLM. It means that the numbers that this plasma system can be on and off before the space-vehicle fails are very high. This result indicates that this plasma system included in space-vehicle structure has the potential to offer the maximum thermal life for UD CF/EP. The ranking of power supplies for imposing the longest to shortest thermal fatigue life on UD CF/EP in spacecraft is indicated as follows:

(1) MHD power supply
(2) GenCore Fuel Cell
(3) Hydrogen-Oxygen Fuel Cell
(4) PEM Fuel Cell
(5) PEMFC and DMFC
(6) PA Fuel Cell
(7) Alkaline Fuel Cell

Consequently, it appears that MHD power supply can be the best candidate for equipping space-vehicles with plasma radiation shield and plasma propulsion systems in manned-space missions. Because the thermal cycles to failure generated by this power supply is maximum for UD CF/EP which creates the longest thermal fatigue life for the space craft made with UD CF/EP.

In comparing ECCM and CSLM, it appears that CSLM is in close agreement with ECCM in terms of prediction of thermal cycle numbers to failure for UD CF/EP. Thus, it seems that the theory of steady and linear region in "ILSS-Thermal cycle numbers" relation is approximately correct. Nevertheless, in conditions in which ΔT_{FC} is greater than ΔT_{LEO}, the difference between the thermal cycle numbers to failure derived by methods ECCM and CSLM increases. This is the nature of CSLM which indicates some kind of warning by decreasing the cycle numbers to failure when the temperature variation in each thermal cycle for power supply is greater than temperature variation in each thermal cycle in LEO. Hence, this can be considered as an advantage of this method due to safety consideration. The opposite of this also occurs. In conditions where the temperature variation in each thermal cycle for fuel cell is less than the temperature variation in each thermal cycle in LEO, the

Thermal Fatigue Cycle Numbers derived by CSLM (blue color) and ECCM (red color)
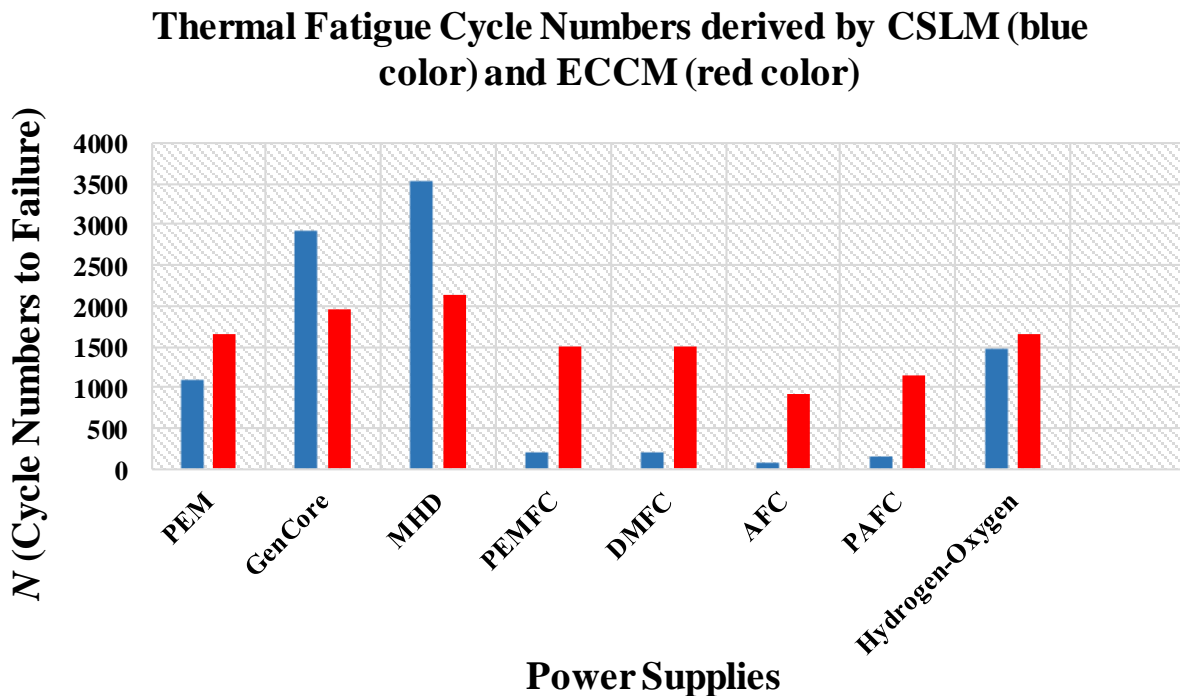
Figure 4. Thermal fatigue cycle numbers to failure (*N*) derived by ECCM (red color) and CSLM (blue color) for UD CF/EP exposed to different power supplies thermal cycles.

number of thermal cycles to failure derived by CSLM is more than that for ECCM. Nevertheless, the average difference for the thermal cycles to failure for UD CF/EP derived by ECCM is 32.2 % higher than that for CSLM. As a result, based on these calculations, it appears that a safety factor of about more than 1.4 is recommended to derive the thermal cycles to failure for UD CF/EP subjected to different power supplies of thermal cycles.

Conclusion

In the study, by using new equations, thermal fatigue life of UD CF/EP which can be used in space-vehicles exposed to different fuel cells or power supplies thermal cycles is derived. For this purpose, new CSLM is applied. The comparison between the new CSLM and ECCM methods has shown that the new CSLM has a close result with ECCM. Hence, based on the results obtained for thermal cycles to failure for UD CF/EP which is subjected to different magnet fuel cells thermal cycles that generate plasma radiation shield and plasma propulsion with both methods, the theory of steady-linear regions for ILSS as a function of thermal cycles is approximately correct. Furthermore, the behavior of CSLM for decreasing the number cycles to failure in conditions where ΔT_{FC} is higher than ΔT_{LEO} is a very important advantage and can be considered as an alert in

failure hazard condition for the space-vehicle. This prediction can contribute to estimate the thermal cycles to failure for UD CF/EP with higher safety and reliability factor. Moreover, according to the results obtained by CSLM and ECCM, MHD appears to be the safest magnet power supply for UD CF/EP space-vehicles' structures. Finally, based on the results obtained with the new CSLM, a minimum safety factor of 1.4 for predicting the thermal cycles to failure for UD CF/EP is recommended.

Symbol definition

ILSS, Inter-laminar shear strength; **ILSS$_0$,** inter-laminar shear strength at zero thermal cycles (maximum ILSS for UD CF/EP); **ILSs$_{max}$,** maximum inter-laminar shear stress; **Δα,** difference of axial coefficients of thermal expansion between carbon fiber and epoxy; **ΔT$_{max}$,** maximum temperature variation between stress-free temperature in UD CF/EP and ambient temperature; **G$_{max}$,** maximum shear modulus in axial direction (carbon fiber's axial shear Modulus); **α$_{carbon\ fiber}$,** carbon fiber's axial coefficient of thermal expansion; **α$_{epoxy}$,** epoxy's axial coefficient of thermal expansion; **N,** cycle numbers to failure; **N$_{steady}$,** Cycle Numbers for Steady-Region; **T$_f$,** UD CF/EP's failure temperature; **ΔT,** temperature variation; **ΔT$_{LEO}$,** temperature variation in each thermal cycle in low earth orbit; **ΔT$_{FC}$,** temperature variation in

each thermal cycle in fuel cell or power supply;

CONFLICT OF INTERESTS

The authors have not declared any conflict of interests.

REFERENCES

Anvari A (2014). Fatigue life prediction of unidirectional carbon fiber/epoxy composite in Earth orbit. International Journal of Applied Mathematics and Mechanics 10(5):58-85.

Anvari A (2017b). Crack growth as a function of temperature variation in carbon fiber/epoxy. Journal of Chemical Engineering and Materials Science 8(3):17–30.

Anvari A (2017a). Fatigue Life Prediction of Unidirectional Carbon Fiber/Epoxy Composite on Mars. Journal of Chemical Engineering and Materials Science 8(8):74-100.

Anvari A (2017c). Thermal fatigue life of carbon nanotube wire and unidirectional carbon fiber/epoxy composite (UCFEC) in earth orbit. Journal of Chemical Engineering and Materials Science 8(8):101-111.

Anvari A (2018). Thermal Life of Carbon Structures; From the Earth to after the Titan. International Journal of Aerospace Engineering. In press.

Birek L, Molitorys S (2009). Hydrogen fuel cell emergency power system. Master's thesis, School for Renewable Energy Science, University of Iceland and University of Akureyri.

Cucinotta FA, Kim MHY, Ren L (2005). Managing Lunar and Mars Mission Radiation Risks-Part I: Cancer Risks, Uncertainties, and Shielding Effectiveness. NASA/Technical Report-213164.

Diaz FC, Seedhouse E (2017). To Mars and Beyond, Fast! How Plasma Propulsion will Revolutionize Space Exploration. Springer International Publishing Switzerland. Published in association with Praxis Publishing, Chichester, UK.

Fuel Cell Handbook (2004). U.S. Department of Energy. Morgantown, West Virginia 26507-0880. Seventh Edition.

Giannadakis K, Varna J (2009). Effect of thermal aging and fatigue on failure resistance of aerospace composite materials. 5th International EEIGM/AMASE/FORGEMAT conference on Advanced Materials Research, IOP Conference Series: Materials Science and Engineering 5:012020:1-9.

Giorgi L, Leccese F (2013). Fuel cells: technologies and applications. The Open Fuel Cells Journal 6:1-20

Horneck G, Comet B (2006). General human health issues for Moon and Mars missions: Results from the HUMEX study. Advances in Space Research 37:100-108.

Jakupca I (2018). Fuel cell research and development for Earth and space applications. Department of Energy. (NASA) Annual Merit Review, 14 June 2018.

Karadeniz ZH, Kumlutas D (2007). A numerical study on the thermal expansion coefficients of fiber reinforced composite materials. Master of science Thesis in mechanical engineering, Energy program, Dokuz Eylul University.

Levy RH, French FW (1967). The Plasma Radiation Shield: Concept, and Applications to Space Vehicles. NASA-George C. Marshal Space Flight Center. AVCO Everett Research Laboratory, Massachusetts.

Levy RH, French FW (1968). Plasma Radiation Shield: Concept and Applications to Space Vehicles. Journal of Space-craft 5(5):570-577.

Park SY, Choi HS, Choi, WJ, Kwon H (2012). Effect of vacuum thermal cyclic exposures on unidirectional carbon fiber/epoxy composites for low earth orbit space applications. Composites: Part B. 43:726-738.

Pasachoff JM (1993). From the Earth to the Universe. Part 2: The Solar System, 11 Mars, Saunders College Publishing, Williamstown, Massachusetts, Fourth Edition, pp. 190-203.

Rahman MS, Riadh RR, Paul S (2015). Investigate the output behavior of Alkaline Fuel Cell's (AFC's) parameters: flow rate and supply pressure. Electrical and Electronics Engineering: An International Journal 4(4):99-118.

Schulze-Makuch D, Davies P (2010). To Boldly Go: A One-Way Human Mission to Mars. Journal of Cosmology 12:3619-3626.

Shin KB, Kim CG, Hong CS, Lee HH (2000). Prediction of failure thermal cycles in graphite/epoxy composite materials under simulated low earth orbit environments. Compos Part B: Eng. 31:223-235.

Vasquez A, Varanauski D, Clark R (2017). Analysis and test of a proton exchange membrane fuel cell power system for space power applications. NASA Johnson space center. Houston, Texas 77058-77059.

Warshay M, Prokopius PR (1989). The fuel cell in space: yesterday, today and tomorrow. NASA Technical Memorandum 102366. Lewis Research Center. Cleveland, Ohio.

Zimcik DG, Wertheimer MR, Balmain KB, Tennyson RC (1991). Plasma-Deposited Protective Coatings for Spacecraft Applications. Journal of Spacecraft 28(6):652-657.